

# Novel Grafted Nafion Membranes for Proton-Exchange Membrane Fuel Cell Applications

M. S. Mohy Eldin,<sup>1</sup> A. A. Elzatahry,<sup>1</sup> K. M. El-Khatib,<sup>2</sup> E. A. Hassan,<sup>3</sup> M. M. El-Sabbah,<sup>3</sup>  
M. A. Abu-Saied<sup>1</sup>

<sup>1</sup>Polymer Materials Research Department Advanced Technologies and New Materials Research Institute, Mubarak City for Scientific Research and Technology Applications, New Borg El-Arab City, Alexandria 21934, Egypt

<sup>2</sup>Pilot Plant Department, Engineering Division, National Research Center, Dokki, Giza, Egypt

<sup>3</sup>Department of Chemistry, Faculty of Science, Al-Azhar University, Cairo, Egypt

Received 11 February 2010; accepted 8 April 2010

DOI 10.1002/app.32613

Published online 20 July 2010 in Wiley Online Library (wileyonlinelibrary.com).

**ABSTRACT:** Novel poly(glycidyl methacrylate)-grafted Nafion–phosphoric acid membranes for direct-oxidation methanol fuel cells were prepared with a potassium persulfate chemical initiation system for the first time. The introduced epoxy groups were converted to amine groups through a reaction with ethylenediamine, which consequently doped with phosphoric acid ( $-\text{PO}_3\text{H}$ ) groups. The latter significantly contributed to enhancing the ion-exchange capacity, mechanical properties, and thermal stability. Factors affecting the modification steps were studied. Changes in the chemical and morphological structure were verified through Fourier transform infrared spectroscopy, TGA, and scanning electron microscopy characterization. Various grafting percentages (GP%'s) up to 32.31% were obtained. As a result, the thickness of the grafted mem-

branes increased. Furthermore, the methanol permeability of the modified membranes was reduced with increasing grafted polymer content compared with that of the Nafion membrane. An 83.64% reduction in the methanol permeability was obtained with a polymer grafted content of 18.27%. Finally, the efficiency factor for all of the modified Nafion membranes was enhanced compared with that of Nafion. A fourfold improvement was obtained with membranes with a GP% of 18.27% as a maximum value. Such promising results nominate the used technique as a one for the improvement of Nafion membrane efficiency. © 2010 Wiley Periodicals, Inc. *J Appl Polym Sci* 119: 120–133, 2011

**Key words:** fluoropolymers; functionalization of polymers; graft copolymers; ion exchangers; membranes

## INTRODUCTION

The principle of the fuel cell dates back to well before the advent of the internal combustion engine. In other words, whereas water can be split into its constituent components, hydrogen and oxygen, through the application of an electric current, the idea behind a fuel cell is essentially the reverse of this process.<sup>1</sup> The fuel cell designs by Francis T. Bacon<sup>2</sup> were eventually chosen by NASA for powering its Apollo mission and the space shuttle orbiters. Although fuel cells were used in the 1950s and 1960s as part of NASA's space program, more practical applications of this process were abandoned by some major companies because the cost of the tech-

nology is higher than those of conventional power-generation technologies. The development of fuel cells since the 1970s has been characterized by the elimination of diffusion limitations in electrode structures and improvements in lifetime. The cost per kilowatt of energy produced in a fuel cell has come down by a factor of 10 over the past 5 years, and specific power outputs of fuel cells have increased dramatically in 20 years. The leading fuel cell companies have reached a point in their advancement of the technology when they have begun to say that fuel cells could soon match the cost of existing technology.<sup>3</sup> Important characteristics enable fuel cells to become a revolutionary technology that could replace the existing technology. According to the application of the fuel cell, the desired number of unit cells, consisting of a membrane electrode assembly and bipolar plate, constitute a fuel cell stack. Thus, the fuel cell system can be made to order to customer specifications with ease. Direct-oxidation methanol fuel cell (DMFC) systems, based on a solid polymer electrolyte in the form of a polymer electrolyte membrane fuel cell, offer a simple and compact design as the methanol is fed directly into the fuel cell as the fuel. The DMFC system is thought to be an attractive power

Correspondence to: M. S. M. Eldin (mohyeldinmohamed@yahoo.com).

Contract grant sponsor: Mubarak City for Scientific Research and Technology Applications; contract grant number: E 1.1.2007-2012 (part of strategic project "The Preparation and Characterization of Polymer Polyelectrolyte Membranes for Direct Methanol Fuel Cell Application.").

source for a range of applications, including transportation and a portable power source.<sup>4</sup> The structure of the DMFC is the composite of two porous electrocatalytic electrodes on either side of a solid polymer electrolyte membrane, and methanol reformation and electrochemical reactions occur simultaneously in the cell.<sup>5</sup> One of the main components in DMFCs is the electrolyte membrane. DuPont Nafion or other perfluorinated sulfonic acid membranes are widely acknowledged to be good electrolyte membranes because of their high proton conductivity and chemical stability. However, Nafion membranes have some drawbacks:<sup>6-8</sup>

1. Nafion is expensive and difficult to process.
2. There is a strong dependence on the relative humidity in maintaining the proton conductivity of Nafion membranes. This is the reason the proton conductivity decreases with dehydration at high temperatures.
3. It is thermally unstable at high temperatures. This property causes the membrane to physically shrink during high-temperature operation, with subsequent poor contact and proton conductivity between the membrane and the electrodes.
4. It has a high methanol permeability, which not only wastes fuel but also reduces cell performance for application in DMFCs.

A number of researchers have dealt with such problem using different strategies to block the channels through the pores of the membranes by some methanol-repealing species.<sup>9-17</sup> The grafting of Nafion with selected polymers has been presented as one of these strategies.<sup>9,10</sup> Sauk et al.<sup>9</sup> grafted styrene onto Nafion 115. The Nafion-grafted polystyrene was sulfonated in concentrated sulfuric acid (98% H<sub>2</sub>SO<sub>4</sub>). The grafted membranes were characterized by the measurement of their ion-exchange capacities (IECs), ion conductivity, and methanol permeation. The Nafion-grafted poly(styrene sulfonic acid) exhibited a higher ion conductivity and lower methanol permeability than that of Nafion 115. On the other hand, Bae et al.<sup>10</sup> grafted polystyrene molecules onto the surface of a Nafion 117 membrane via the plasma-induced polymerization technique to reduce its methanol permeability in applications involving DMFCs. The cross-linked poly(styrene sulfonic acid) layers that were grafted reduced the methanol permeability of the membranes considerably.

In this article, the grafting of Nafion membranes with a simple chemical initiation system is presented for the first time. We studied the grafting of Nafion membranes with poly(glycidyl methacrylate) (PGMA) with a potassium persulfate (KPS) initiation system by exploring the effects of different factors, such as monomer and initiator concentration, on the grafting process.

Three parameters, namely, the grafting percentage (GP%), grafting efficiency (GE%), and weight conversion (WC%), were monitored. Different GP%'s were obtained and controlled as a result of the variation of the grafting conditions. The introduced epoxy groups of PGMA were subsequently converted into amine groups by the amination process with ethylenediamine (EDA). The amination conditions, such as EDA concentration, reaction time, and temperature were investigated. The phosphorylation of the produced amine groups to induce ionic conductivity to overcome some of the original lost as a result of the grafting process was conducted as a last step of the modification process of the Nafion membranes. The phosphorylation conditions, such as *ortho*-phosphoric acid concentration, reaction time, and temperature, were investigated to determine the optimum modification conditions. To follow up changes resulting from the modification process, different characteristics and measurements were evaluated, namely, the water uptake, methanol uptake, dimensional changes, tensile strength (TS) of the membrane, membrane thickness changes, IEC, methanol permeability, membrane efficiency, Fourier transform infrared (FTIR) analysis, TGA, and scanning electron microscopy (SEM) analysis.

## EXPERIMENTAL

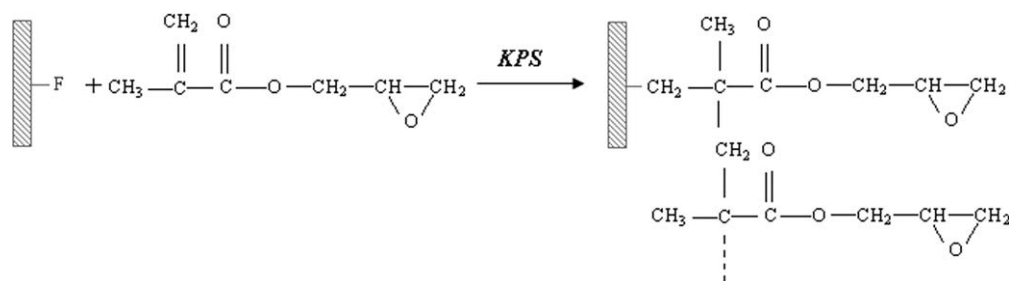
### Materials

Glycidyl methacrylate (GMA; purity = 97%) was obtained from Sigma-Aldrich Chemicals (Switzerland). Nafion 117 was purchased from DuPont. KPS (purity = 99%, molecular weight = 270.31) was obtained from Sigma-Aldrich Chemicals, Ltd. (Germany). Ethyl alcohol absolute (purity = 99.9%) was obtained from El-Nasr Pharmaceutical Co. for Chemicals (Egypt). Sulfuric acid (purity = 95–97%) was obtained from Sigma-Aldrich Chemicals, Ltd. (Germany). Methanol (purity 99.8%) was obtained from Sigma-Aldrich Chemicals, Ltd. (Germany). *ortho*-Phosphoric acid (purity = 85%, extrapure) was obtained from Sigma-Aldrich Chemicals, Ltd. (Germany). EDA (purity = 99%) was obtained from Loba Chemie (India). Hydrochloric acid (purity = 30–34%) was obtained from El-Nasr Pharmaceutical Co. for Chemicals. Sodium chloride (purity = 99.5%, molecular weight = 58.44) was obtained from Sigma-Aldrich Chemicals, Ltd. (Germany). Hydrogen peroxide (purity = 35%) was obtained from El-Nasr Pharmaceutical Co. for Chemicals.

### Methods

#### Membrane preparation

*Membrane treatment.* Commercial Nafion 117 membranes (DuPont) were treated according to standard



**Scheme 1** Mechanism of the Nafion grafting.

membrane cleaning procedures.<sup>18</sup> Briefly, the Nafion 117 membranes were boiled at 80°C for 1 h in a 5% H<sub>2</sub>O<sub>2</sub> solution, deionized water, a 0.5M H<sub>2</sub>SO<sub>4</sub> solution, and again in deionized water. Finally, the membranes were air-dried in an air oven at 30°C.

**Grafting process.** Grafting was carried out with different monomer concentrations (8–20% v/v) dissolved in KPS solutions (0.004–0.012M) with differ-

ent composition of ethanol–water. The grafting process was conducted at different temperatures (35–65°C) in a water bath for different reaction times (1–5 h; Scheme 1). The grafting process was monitored through the evaluation of different grafting parameters, namely, GP%, GE%, and WC%. These parameters were calculated with the following equations:<sup>19</sup>

$$\text{GP}\% = \frac{\text{Weight of the grafted membrane after extraction} - \text{Weight of the original membrane}}{\text{Weight of the original membrane}} \times 100 \quad (1)$$

$$\text{GE}\% = \frac{\text{Weight of the grafted membrane} - \text{Weight of the original membrane}}{\text{Weight of the grafted polymers} + \text{Weight of the homopolymer}} \times 100 \quad (2)$$

$$\text{WC}\% = \frac{\text{Weight of the grafted polymer} + \text{Weight of the homopolymer}}{\text{Weight of the used monomer}} \times 100 \quad (3)$$

**Amination process.** The epoxy groups of the PGMA chains were reacted with EDA at different concentrations (1–6% v/v) in water at different temperatures (25–65°C) in a water bath and for different time intervals (2–10 h; Scheme 2).

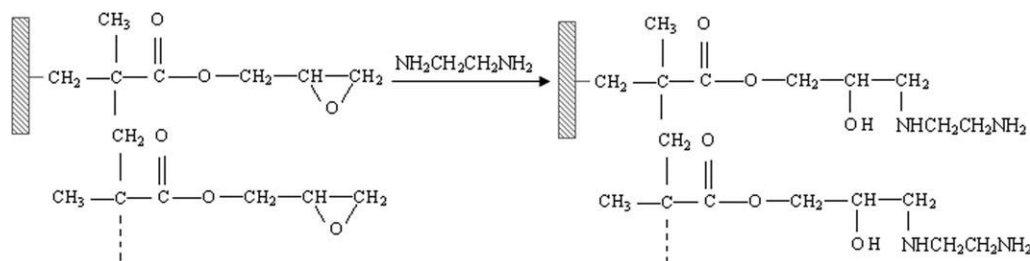
**Phosphorization process.** Phosphorization was carried out with different *ortho*-phosphoric acid concentrations (1.5–7.5% v/v) dissolved in water at different temperatures (25–65°C) in a water bath for different

time intervals (2–10 h); this was followed by membrane washing with distilled water.

#### Membrane characterization

**Water uptake (W%).** For membrane previously immersed in distilled water at room temperature for 24 h, the surface was dried by wiping with filter paper and weighing. The obtained results were the average of three samples.<sup>20</sup>

$$W_{\text{H}_2\text{O}}\% = \frac{\text{Weight of the membrane (g)} - \text{Weight of the dry membrane (g)}}{\text{Weight of the dry membrane (g)}} \times 100 \quad (4)$$



**Scheme 2** Mechanism of the PGMA-g-Nafion membrane amination process.

*Methanol uptake (W%).* For membrane previously immersed in pure methanol at room temperature for 24 h, the surface was dried by wiping with filter

$$W_{\text{MeOH}}\% = \frac{\text{Weight of the membrane (g)} - \text{Weight of the dry membrane (g)}}{\text{Weight of the dry membrane (g)}} \times 100 \quad (5)$$

*IR spectrophotometric analysis.* Analysis of IR spectroscopic charts to investigate the chemical structure of the ungrafted and modified membranes having different GP%'s was carried out with an FTIR spectrophotometer (Shimadzu FTIR-8400 S, Japan).

*Thermogravimetric analysis (TGA).* TGA of the ungrafted and modified membranes having different GP%'s was carried out with a thermogravimetric analyzer (Shimadzu TGA-50).

*SEM analysis.* Scanning of the ungrafted and modified membranes was carried out with energy-dispersive X-ray analysis (JEOL JSM 6360LA, Japan).

*IEC.* The IEC of the membranes was determined with acid–base titration. Weighed samples were immersed in 20 cm<sup>3</sup> of a 2M NaCl solution for at least 12 h at room temperature. The solution was then titrated with a NaOH solution of known concentration. IEC was calculated as follows:

$$\text{IEC}(\text{mequiv/g}) = n(\text{mmol/cm}^3) \times v(\text{cm}^3)/w(\text{g}) \quad (6)$$

where  $n$ ,  $v$ , and  $w$  are the concentration of the NaOH solution, the titer of the NaOH solution, and the weight of the sample, respectively.<sup>21</sup>

*Methanol permeability.* Methanol permeability measurements were carried out with a homemade glass diffusion cell that consisted of two cylindrical glass compartments (compartment A for the feed and compartment B for the permeate) separated by a membrane. A schematic representation of the methanol diffusion cell is presented in Scheme 3. Compartment A was filled with 15 wt % methanol (volume of compartment A = 125 mL), and compartment B was filled with deionized water [volume of the water compartment ( $V_B$ ) = 120 mL]. Both the feed and the permeate solutions were kept under continuous stirring conditions by magnetic stirrers. To determine the methanol permeability of each membrane, liquid samples of 100  $\mu\text{L}$  were taken from the permeate with a syringe at prescribed time intervals. The liquid samples were analyzed with a calibrated gas chromatograph (GC-17 A, Shimadzu).

*Methanol permeability calculations.* The methanol permeability ( $P$ ) was determined for each membrane sample as follows: Methanol diffusion was established across the membrane due to a concentration gradient. The concentration of methanol in the

permeate compartment is given by eq. (7), as stated elsewhere:<sup>22</sup>

$$\frac{V_B dC_B}{dt} = A \frac{DK}{L} C_A \quad (7)$$

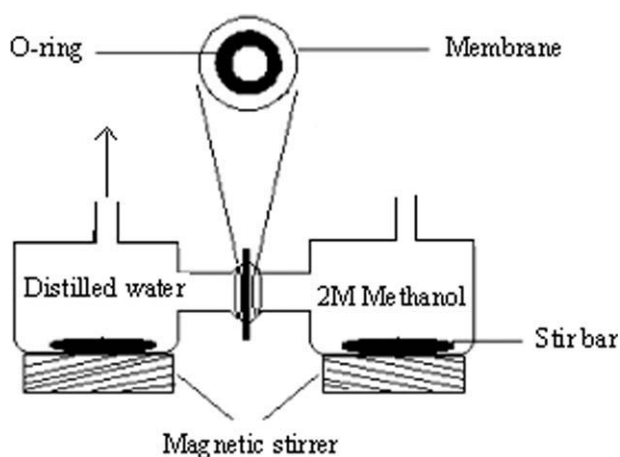
where  $C_B$  is the concentration of methanol in the permeate (water) compartment at time  $t$ ,  $C_A$  is the concentration of methanol in the feed compartment,  $A$  is the membrane cross-sectional area,  $L$  is the membrane thickness,  $D$  is the methanol diffusivity, and  $K$  is the partition coefficient. Equation (8) can be solved to give

$$C_B(t) = \frac{A DK}{V_B L} C_A (t - t_0) \quad (8)$$

where  $t_0$  is the time lag, which is explicitly related to  $D$  ( $t_0 = L^2/6D$ ). Because the methanol permeability is defined as the product of  $D$  through the membrane and the partition coefficient, that is,  $P = DK$ , eq. (9) can be rewritten as follows:

$$C_B(t) = \frac{A P}{V_B L} C_A (t - t_0) \quad (9)$$

The methanol permeability is calculated from the linear relationship of the concentration change of  $C_B$  versus time according to the following expression:



**Scheme 3** Glass diffusion cell for the methanol permeability measurements.

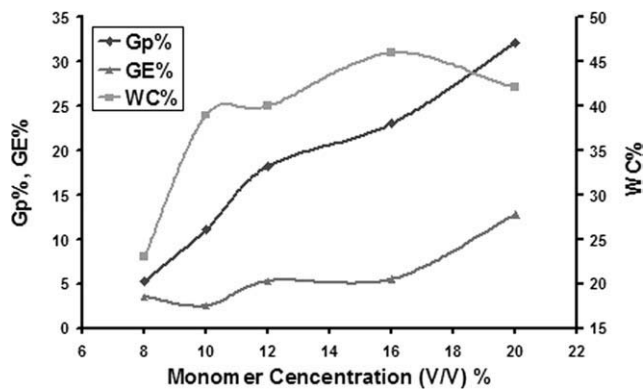


**Figure 1** Effect of the monomer concentration on GP%, GE%, and WC% (conditions: 0.01M KPS, 1 : 1 ethanol-water ratio, 55°C, and 4 h).

$$P = \alpha \frac{V_B L}{A C_A} \quad (10)$$

where  $\alpha$  is the slope of the linear plot of  $C_B$  versus time.

*Calculation of the membrane efficiency.* Because DMFC application requires membrane quality that attains a high proton conductivity and methanol impermeability, the membrane performance evaluation can be obtained with the following expression:<sup>22</sup>

$$\Phi = \frac{\sigma}{P} \quad (11)$$

where  $\Phi$  is a parameter that evaluates the overall membrane performance in terms of the ratio of the ionic conductivity ( $\sigma$ ) to the methanol permeability. However, in this work, the IEC was an indicator for ionic conductivity, and we compared the efficiency modified of the composite membranes in respect to the virgin membrane by IEC to the methanol permeability ratio according to the following equation:

$$\Phi = \frac{IEC}{P} \quad (12)$$

where  $\Phi$  is the efficiency factor.

*TS measurement.* TS is a measure of the resistance of a sample to direct tension. It is defined as the force required to break a strip of sample that has a specified length and a width of 10 mm. A Lloyd Instruments LR 10K was used for TS measurements:

Breaking length (m) = TS (kg) ×

Length of the strip (m)/Weight of the strip (kg)

where 1 kg/15 mm = 3.73 lb/in. and

Zero – span breaking length = Breaking load (kg) ×  
200,000/[Basis weight/in.<sup>2</sup> × 3]

where the sample size is 1 × 5 cm<sup>2</sup>.

*Dimensional changes ( $\Delta A\%$ ).* After the membranes were immersed into deionized water or pure methanol at room temperature for 24 h,  $\Delta A\%$  was calculated from following equation:

$$\Delta A\% = \frac{A - A_0}{A_0} \times 100 \quad (13)$$

where  $A_0$  and  $A$  are the areas of membrane before and after the soaking treatment, respectively.

## RESULTS AND DISCUSSION

### Membrane preparation

Grafting process

*Effect of the monomer concentration.* The diffusability of the monomers into the polymer matrix had a great influence on the grafting process. The effect of the monomer concentration on GP%'s, GE%, and total WC% was investigated. Figure 1 shows that an increase in the monomer concentration clearly increased GP% and GE%. The maximum GP% and GE% were obtained with a 20% GMA solution, whereas the WC% reached maximum value at 16% GMA and then tended to decrease slightly with further increasing GMA. These observations were attributed to the following explanations. Increases in the monomer concentration up to 20% facilitated the diffusability of the monomer toward the initiated sites on the chains of the Nafion membranes, which consequently increased the grafting yield.

*Effect of the initiator concentration.* Figure 2 shows the effect of the variation of KPS concentration on the

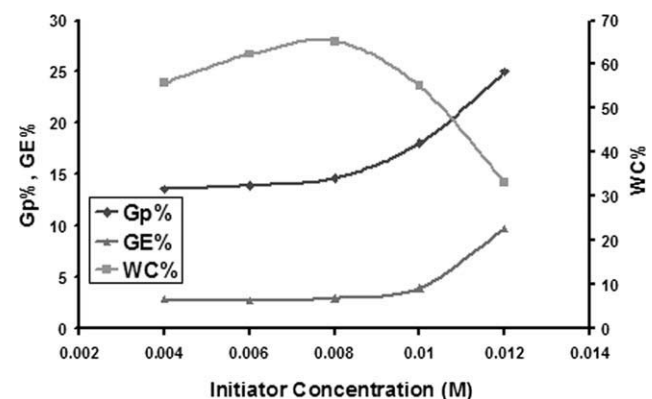


**Figure 2** Effect of the initiator concentration on GP%, GE%, and WC%. (conditions: 12% GMA, 1 : 1 ethanol-water ratio, 55°C, and 4 h).

studied grafting parameters. It was clear that increases in the initiator concentration from 0.004 to 0.012M were accompanied by a significant increase in GP%. This may have been due to an increase in the number of the formed free radicals, as a result of the increase in the initiator concentration, which resulted in an increase of the diffusive numbers of the formed free radicals inside the membranes in benefit of GP%. GE% of the system followed a relatively similar trend, despite its low value. On the other hand, WC% practically increased with increasing initiator concentration up to 0.008M. Beyond 0.008M, the conversion of the monomer dropped sharply to reach a minimum value of 33%. This behavior was explained by the favoring of the termination process in this range of initiator concentrations.

*Effect of the grafting temperature.* The effect of the variation of the polymerization temperature on the grafting parameters is illustrated in Figure 3. Substantial increases in GP% and GE% were observed with variation of the temperature from 35 to 55°C. This enhancement in the grafting of GMA onto the Nafion membranes with increasing polymerization temperature might have been due to the following favorable effects of temperature on

1. The diffusion of GMA from the solution phase to the swellable Nafion phase.
2. Increasing the solubility of the monomer.
3. Increasing the rate of thermal dissociation of KPS and, hence, the GMA rate of free-radical formation on the membrane backbone.
4. Formation and propagation of grafted chains.

The net effect of all such factors led to a high grafting yield with increasing polymerization temperature. Further increases in the polymerization temperature beyond 55°C resulted in a decrease in both GP% and GE%. This could have been due to

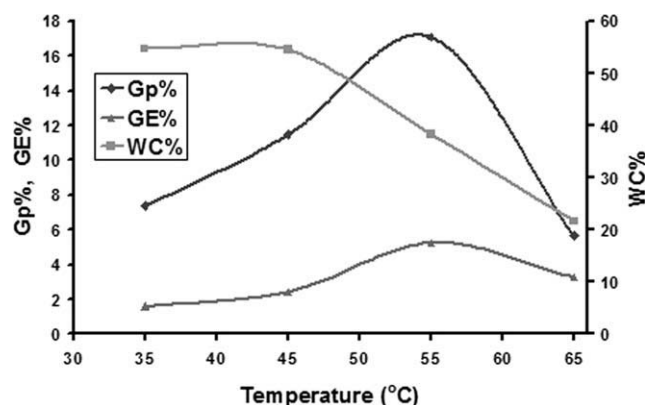


**Figure 3** Effect of the grafting temperature on GP%, GE%, and WC%. (conditions: 12% GMA, 1 : 1 ethanol-water ratio, 0.01M KPS, and 4 h).

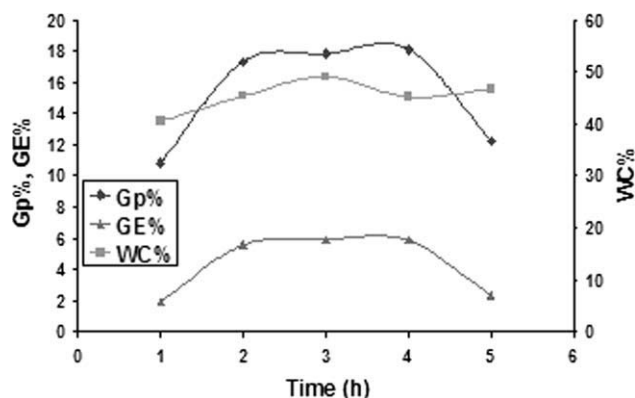


**Figure 4** Effect of the grafting time on GP%, GE%, and WC% (conditions: 12% GMA, 1 : 1 ethanol-water ratio, 0.01M KPS, and 55°C).

the inhibition of polymer formation, as was clear from the depression of WC%. The termination of the formed free radicals was the reasonable cause.

*Effect of the grafting time.* The effect of the variation of grafting time on the grafting parameters is illustrated in Figure 4. The results reveal that increasing the grafting time from 1 to 5 h increased GP% and GE% in the same manner to reach maximum values after 4 h of grafting time. This kind of behavior may have been due to the combination of two processes. The first was an increase the number of formed free radicals in both the monomer solution phase and the polymer solid phase. Simultaneously, in parallel, the amount of diffused monomer in to the polymer phase increased during postgrafting time. The combination of the two processes led finally to increases in both GP% and GE%. On the other hand, further increases in the reaction time to 5 h negatively affected both GP% and GE%. This could be explained by the favoring of homopolymer formation over the grafting process. A diffusion barrier against monomer diffusion into the polymer matrix was created because of the hydrophobic nature of the precipitated homopolymer onto the surface of the membrane. This directly affected the values of both GP% and GE% during the postgrafting time.

*Effect of the solvent composition.* Data illustrating the effects of various solvent compositions on the grafting parameters are shown in Figure 5. GP% and GE% increased linearly with ethanol content to reach maximum values in a 50% ethanol aqueous solution and then tended to decrease. This could be explained by the increasing solubility of GMA, which in turn, facilitated its diffusion into the polymer matrix. In addition, ethanol acted as reducing agent, which facilitated the process of KPS oxidation to form free radicals. The drop in all grafting parameters with a solvent composition of ethanol over 50% may have been due to a reduction of KPS solubility,

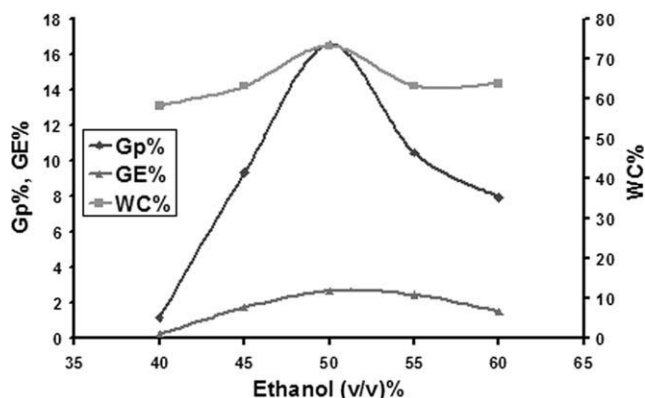


**Figure 5** Effect of the variation of solvent composition on GP%, GE%, and WC% (conditions: 12% GMA, 4 h, 0.01M KPS, and 55°C).

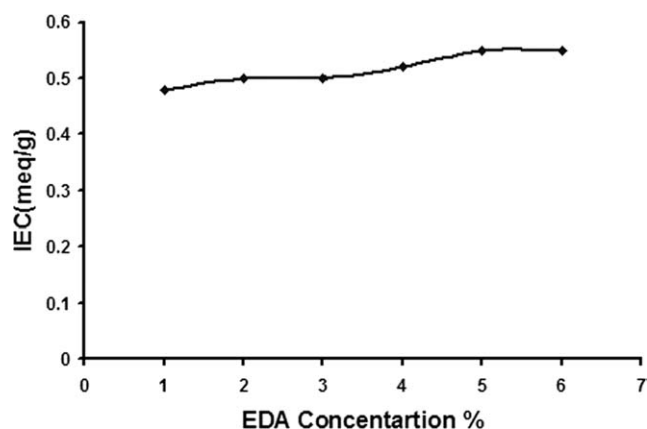
which in turn, reduced the number of formed free radicals.

#### Amination process

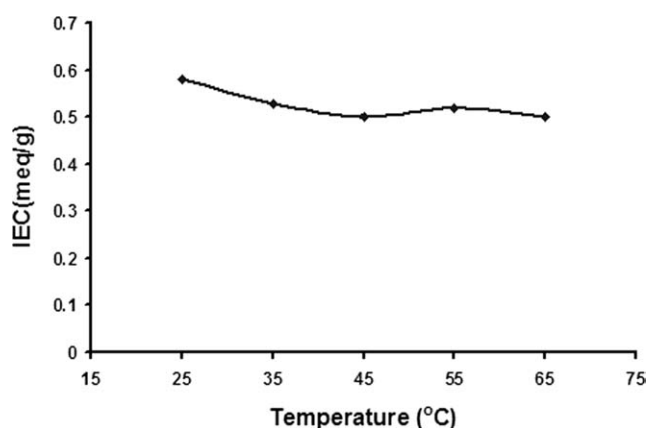
*Effect of the EDA concentration.* The effects of various EDA concentration on IEC are shown in Figure 6. The figure shows that there was a small increment of IEC with increasing EDA concentration from 1 to 6%. This may have been due to the fact that most of the epoxy groups were aminated with 1% EDA, so a further increase in EDA had no significant effect.

*Effect of the reaction temperature.* The effects of various aminoalkylation temperatures of IEC are shown in Figure 7. As shown in Figure 7, IEC decreased slowly with increasing temperature from 25 to 65°C. This is may be explained on the basis of the hydrophilic nature of the Nafion membrane and its very small thickness, which eliminated the enhancing effect of EDA diffusion because of temperature elevation.

*Effect of the reaction time.* The effects of various aminoalkylation reaction times on IEC are shown in



**Figure 6** Effect of the variation of EDA concentration on IEC (conditions: GP% = 18%, 8 h, and 25°C).



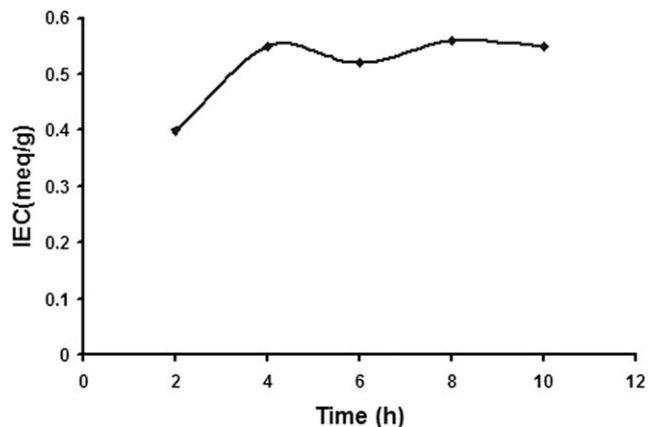
**Figure 7** Effect of the variation of temperature on IEC (conditions: GP% = 18%, 5% EDA, and 8 h).

Figure 8. As shown in Figure 8, IEC increased with increasing time of reaction up to 4 h. Further increases in the amination time had no significant effect. Here again, the hydrophilicity and small thickness of membrane may have caused the described results, in addition to the fact that almost all of the epoxy groups had reacted by 4 h.

#### Phosphorization process

*Effect of the ortho-phosphoric acid concentration.* The effects of various ortho-phosphoric acid concentrations on IEC are shown in Figure 9. As shown in Figure 9, there was an increase in IEC with increasing ortho-phosphoric acid concentration. The maximum IEC was obtained at 6% ortho-phosphoric acid and then tended to level off.

*Effect of the reaction temperature.* The effects of various temperatures on the phosphorization process are shown in Figure 10. As shown in Figure 10, the IEC decreased slowly with increasing temperature from 25 to 65°C. The nonsignificant effect of the reaction



**Figure 8** Effect of the variation of time on IEC (GP% = 18%, 5% EDA, and 25°C).

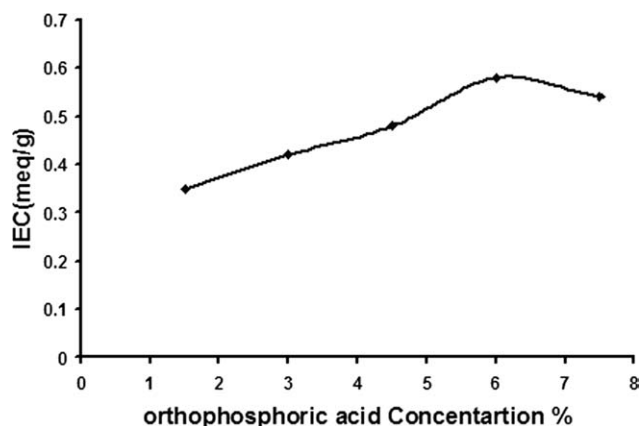


**Figure 9** Effect of the variation of *ortho*-phosphoric acid concentration on IEC (conditions: GP% = 18% and 5% EDA, 25°C, and 8 h or 10 h and 25°C).

temperature could be attributed to the hydrophilicity and small thickness of the Nafion membranes, which eliminated the diffusive enhancement effect of elevation temperature.

*Effect of the time.* The effects of various reaction times on IEC are shown in Figure 11. As shown in Figure 11, IEC increased with increasing reaction time to reach its maximum value after 8 h. The relatively long time needed to reach the maximum IEC, 8 h, may have resulted from the bulk nature of the *ortho*-phosphoric acid groups, which formed clouds on the surface of the membrane and retarded further diffusion of *ortho*-phosphoric acid to reach the terminal amine groups in the polymer bulk.

#### Membrane characterization

*Water and methanol uptakes.* The water content in polymer electrolyte membrane is one of the features of proton transport.<sup>23</sup> Water and methanol uptakes of polymer membranes are directly related to its

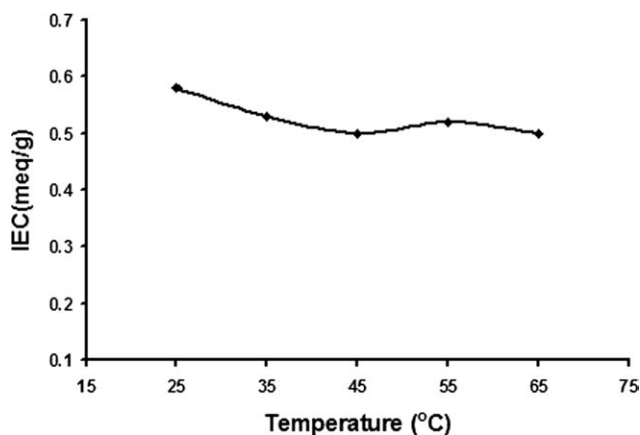


**Figure 10** Effect of the variation of temperature on IEC. (GP% = 18% and 5% EDA, 25°C, and 8 h or 6% *ortho*-phosphoric acid and 10 h).

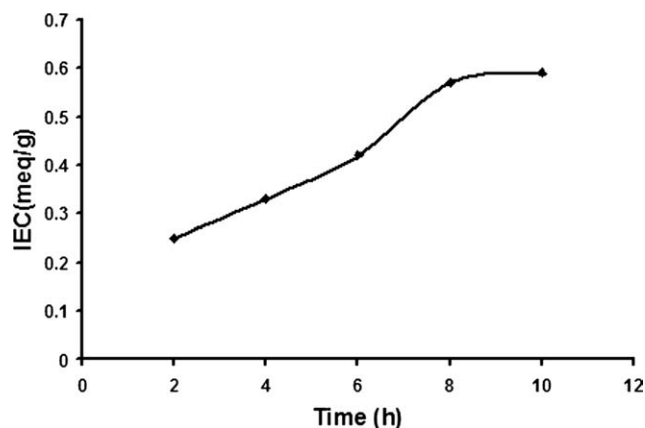


**Figure 11** Effect of the variation of time on IEC (GP% = 18% and 5% EDA, 25°C, and 8 h or 6% *ortho*-phosphoric acid and 25°C).

electrochemical properties for application in DMFCs. The data of the water and methanol uptakes of various grafted Nafion membranes together with that of the ungrafted membrane are presented in Tables I and II.

It is clear from the data tabulated in Tables I and II that the water uptake for the grafted membranes was greater than that of virgin Nafion, and this was not expected from the hydrophobic nature of PGMA. This may have been due to the hydrolysis of the epoxy ring in PGMA with the formation of  $\alpha$ -glycol groups due to acid catalyzed hydrolysis by action of HCl used for the regeneration of the modified membranes to their acid form. After the grafting process, the epoxy ring was reactive for hydrolysis under these conditions,<sup>24</sup> and therefore, a high percentage of the epoxy groups were consumed with the formation of excellent hydrophilic groups (hydroxyl groups), which were responsible for the higher water uptake and higher number of sorbed water molecules.

Also, for the aminated and phosphorized membranes, the amination of the remaining epoxy groups resulted in the formation of amine groups and hydroxyl groups, and they were excellent

**TABLE I**  
Water Uptake Values of the Ungrafted, Grafted, Aminated, and Phosphorized Membranes

GP%	Water uptake of the grafted membrane (%)	Water uptake of the aminated membrane (%)	Water uptake of the phosphorized membrane (%)
0	18.94	—	—
5.27	24.32	17.125	21.01
11.08	24	19.25	22.43
18.27	27.78	23.64	28.82
23.308	38.49	27.71	34.8
32.18	40.16	33.09	37.01



**TABLE II**  
Methanol Uptake Values of the Ungrafted, Grafted, Aminated, and Phosphorized Membranes

GP%	Methanol uptake of the grafted membrane (%)	Methanol uptake of the aminated membrane (%)	Methanol uptake of the phosphorized membrane (%)
0	22	—	—
5.27	34.31	27.87	37.5
11.08	32.04	27.1	36.53
18.27	42.16	30.956	48.03
23.308	50.66	35.518	51.96
32.18	53.126	40.50	60.78

hydrophilic groups, which were responsible for the high water uptake and higher number of sorbed water molecules.<sup>25</sup> The attachment of phosphoric acid groups was confirmed by the IEC measurements for the membranes, which are discussed later.

However, the water uptake for both aminated and grafted membranes was higher than that of virgin Nafion membranes. The increase in methanol uptake for all of the membranes was significant. This was attributed to the hydrogen bonding between the membrane matrix and the methanol molecules.<sup>26</sup>

*Dimensional changes.* The effects of the modification process on the dimensional changes of the modified membranes in methanol and water were tested for all of the modified membranes after they were swollen in water and methanol separately for 24 h. The results show that the dimensional changes of the modified membranes after swelling in methanol or water were significant in comparison with the unmodified membrane. This confirmed that the modification process had an impact effect on the dimensional changes of the modified membranes (Table III and IV).

*Mechanical characterization.* TS and elongation at break were measured on rectangular strips. TS indicates the maximum stress developed in a film during a tensile testing, and elongation at break indicates the capacity of the film to stretch.<sup>27</sup> The

**TABLE III**  
Dimensional Changes in Water for the Ungrafted, Grafted, Aminated, and Phosphorized Membranes

GP%	Dimensional changes of the grafted membrane (%)	Dimensional changes of aminated membrane (%)	Dimensional changes of the phosphorized membrane (%)
0	15	—	—
5.27	20.37	15	20
11.08	21.25	16.66	22.22
18.27	33.58	19.736	30.26
23.308	36.11	29.192	34.16
32.18	30.5	37.09	35

**TABLE IV**  
Dimensional Changes in Methanol for the Ungrafted, Grafted, Aminated, and Phosphorized Membranes

GP%	Dimensional changes of the grafted membrane (%)	Dimensional changes of the amination membrane (%)	Dimensional changes of the phosphorized membrane (%)
0	35	—	—
5.27	45.15	34.056	36.9
11.08	40.30	33.4921	46.66
18.27	53.78	46.762	51.31
23.308	54.16	45.285	62.11
32.18	56	49.31	66.43

tensile properties of the ungrafted and different percentage grafted membranes were measured and are recorded in Table V. These were determined from the critical breaking point of the stretching test pieces.

The effect of the force on the elongation of the membrane was observed as a positive result because the elongation of the membrane increased as a result of phosphorization. This means that phosphorization of the membrane induced more elasticity compared with the ungrafted Nafion membrane. In general, an improvement in the mechanical properties of the modified Nafion membranes was obtained.

*Membrane thickness changes.* Because of the grafting of the PGMA onto the Nafion membranes, the thickness of the membranes was changed. Figure 12 shows the change in the membranes thickness as measured by a micrometer against the grafting percents. It was clear from the graph that the thickness of the grafted membranes increased with increasing GP%. This may have been due to the incorporation of the PGMA chains onto the matrix of the Nafion membrane.

*IR spectrophotometric analysis.* Figure 13 illustrates the FTIR spectra for the ungrafted, grafted, aminated, and phosphorized Nafion membranes. The appearance of the characteristic absorption band for  $\text{C}=\text{O}$  at  $1724\text{ cm}^{-1}$  and three characteristic bands for epoxy rings at  $1238\text{--}1255$ ,  $840$ , and  $750\text{ cm}^{-1}$  [Fig. 13(b)] provided evidence for the occurrence of the grafting process of PGMA.<sup>28</sup> The opening of the epoxy rings through the amination process was proven through the appearance of characteristic bands

**TABLE V**  
TS and Elongation of the Ungrafted Nafion Membrane and Phosphorized Nafion Membrane

GP%	TS (N)	Elongation (mm)
0	18.125	12.218
18.27	46.25	16.412
23.08	56.09	20.05

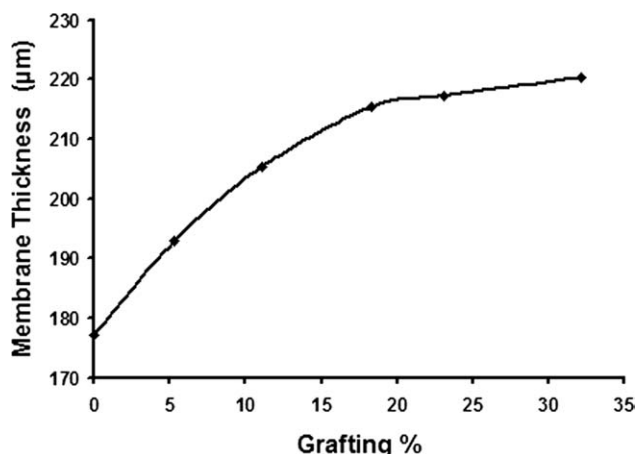


Figure 12 Effect of GP% on the thickness of the grafted membranes.

for the NH<sub>2</sub> group at 3357 cm<sup>-1</sup>. The remaining characteristic bands for epoxy rings were indicated in the complete amination reaction [Fig. 13(c)]. When phosphoric acid was added, a very broad

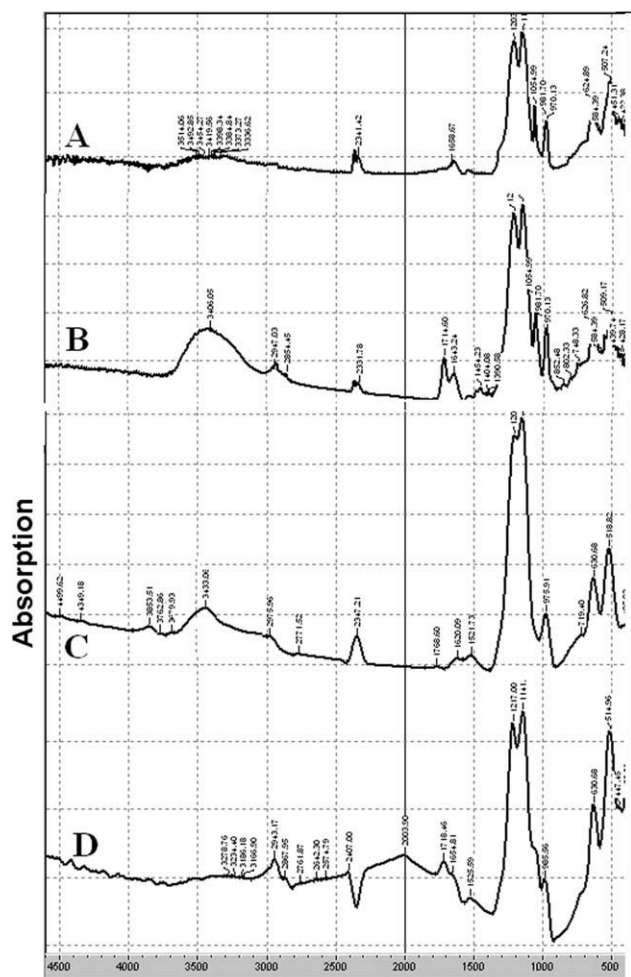


Figure 13 FTIR spectrum of the (A) original Nafion membrane, (B) grafted membrane, (C) aminated Nafion membrane, and (D) phosphorized Nafion membrane.

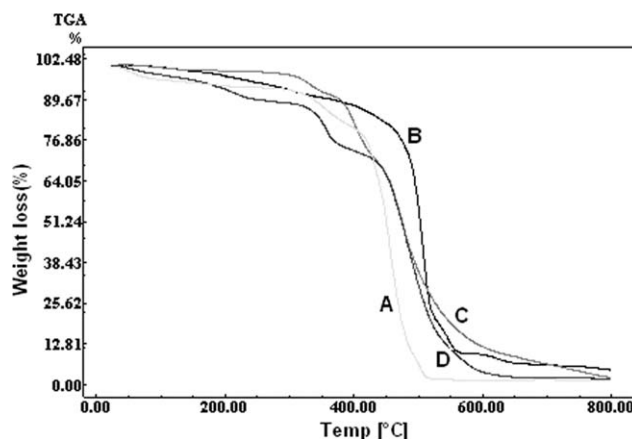
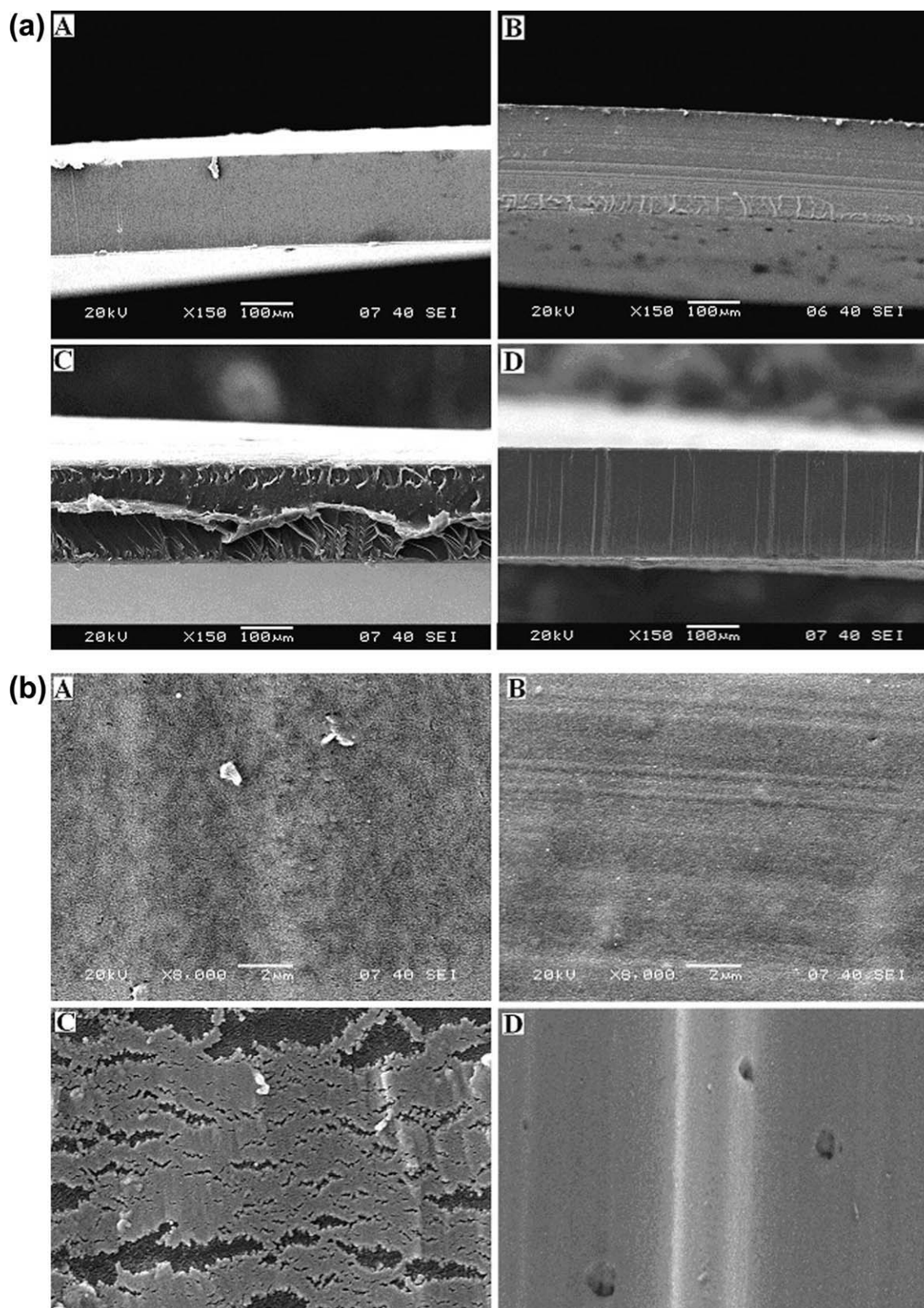


Figure 14 TGA thermographs of the (A) original Nafion membrane, (B) grafted membrane (18.27%), (C) aminated membrane, and (D) phosphorized membrane.

absorption band complex appeared in the wave-number range 2500 to 3000 cm<sup>-1</sup>.<sup>28</sup> TGA. Thermal analysis of the PGMA grafted and ungrafted Nafion membranes were carried out by a thermogravimetric analyzer in a nitrogen atmosphere at a heating rate of 20°C/min (Fig. 14). It was abstracted from TGA that PGMA had two consecutive weight loss steps due to the thermal decomposition of PGMA. The first was in the temperature range 160–320°C, and the second was in the temperature range 360–460°C.<sup>29</sup> Two decomposition steps for the virgin Nafion were observed. The initial decomposition step was at 40–100°C, and this was attributed to water loss in the membrane. The second decomposition step happened at 340–550°C because of the thermal decomposition of groups present in the Nafion matrix.<sup>30</sup> Data obtained from TGA provided us with proof of the occurrences of the grafting, amination, and phosphorization processes. At 450°C, the virgin Nafion membrane lost 50% of its weight, whereas the grafted, aminated, and phosphorized membranes lost 14, 35, and 35% of their weights, respectively, at this temperature.

TABLE VI  
Weight Loss Percentage at 550°C of the Ungrafted, Grafted, Aminated, and Phosphorized Membranes

GP%	Weight loss for the grafted membranes (%)	Weight loss for the aminated membranes (%)	Weight loss for the phosphorized membranes (%)
Original Nafion	95	—	—
5.27	89.33	86.49	85.42
11.08	86.87	80.48	78.96
18.27	87.27	79.52	77.12
23.08	85.80	76.87	75.40
32.18	81.86	73.31	67.62



**Figure 15** (a,b) SEM micrographs of the (A) original Nafion membrane, (B) grafted membrane (23.08%), (C) aminated membrane, (D) and phosphorized membrane.

Following up the effect of graft content on the thermal stability of the modified membranes at different steps of modification, we estimated the weight loss

at 550°C for membranes with different graft contents where the Nafion membrane lost almost all of its weight (Table VI).

**TABLE VII**  
IEC for the Ungrafted and Grafted Nafion Membranes

GP%	IEC (mequiv/g)
0	0.90
5.27	0.61
11.08	0.57
18.27	0.55
23.08	0.50
32.18	0.50

It was clear from the data tabulated that the weight loss percentages for all of the modified membranes were less than that of the original Nafion; this indicated that the modified membranes were more thermally stable than the Nafion membrane. In general, the incorporation of PGMA into the Nafion membrane increased its thermal stability.

*SEM analysis.* Figure 15 displays SEM pictures for both the cross sections and surfaces of the ungrafted Nafion, grafted, aminated, and phosphorized membranes. It was clear from the cross-sectional figures that no phase separation was observed because of the modification process [Fig. 15(A)]. It was clear from surface observation that the changes in the structure were a result of the grafting and subsequent amination and phosphorization processes [Fig. 15(B)].

*IEC.* IEC indicates the density of ionizable hydrophilic groups in the membrane matrix; these were responsible for the ionic conductivity of the membranes and, thus, were an indirect approximation of the proton conductivity.<sup>31</sup> This is one of the main requirements for the application of proton-exchange membranes in DMFC applications. Table VII displays the IEC values for the ungrafted and grafted membranes as determined from the acid-base titration method with respect to GP%. For comparison, IEC for the original Nafion (ungrafted) membrane was determined by the same method and under the same conditions.

From the tabulated data, it was clear that IEC of the grafted membranes was less than that of the Nafion membrane (0.9 mequiv/g) as determined in this study. IEC decreased slightly with increasing grafting extent. This may have been due to the consumption of part of the sulfonic groups as sites for initiation of the grafting process. This result was in accordance with other obtained data.<sup>9</sup>

*Methanol permeability measurements.* Low methanol permeability with high ionic conductivity is an important requirement for proton-exchange membranes in DMFCs. The methanol permeability for the phosphorized membranes in comparison with that of the Nafion membrane was determined with a diffusion cell in which the membrane was clamped between two reservoirs of 2M methanol and distilled

water. The concentration of methanol in the water reservoir was followed with gas chromatographic analysis to estimate the methanol permeability for all of the membranes under investigation. The changes in the methanol concentration in the water compartment against the permeation time for all of the membranes are represented graphically in Figure 16.

As shown in Figure 16, it was clear that the methanol concentration in the water compartment for the modified membranes was lower than that for the Nafion membrane. This may have been due to the incorporation of PGMA layers, which could have acted as barriers for methanol crossover into the polymer matrix of the Nafion membrane. The methanol permeability was calculated from the slope of the linear line of methanol concentration versus permeation time. An attempt to establish whether there was a correlation with the amount of PGMA content in the phosphorized modified membranes was made. The results are represented graphically in Figure 17.

As shown in Figure 17, we observed that the Nafion membrane displayed a methanol permeability of  $3.39 \times 10^{-6} \text{ cm}^2/\text{s}$ , which was quite close to that reported by other authors.<sup>32</sup> Also, the methanol permeability of the modified membranes was lower than that of the Nafion membrane, and it decreased with increasing grafted polymer content.

The results show that the methanol permeability decreased by about 66.43%, with respect to the virgin Nafion value, with a grafted polymer content of 11.08%. Consequently, the value of methanol permeability decreased with increasing grafted polymer content until it was reduced by 83.64% with a polymer grafted content of 18.27%. On the other hand,

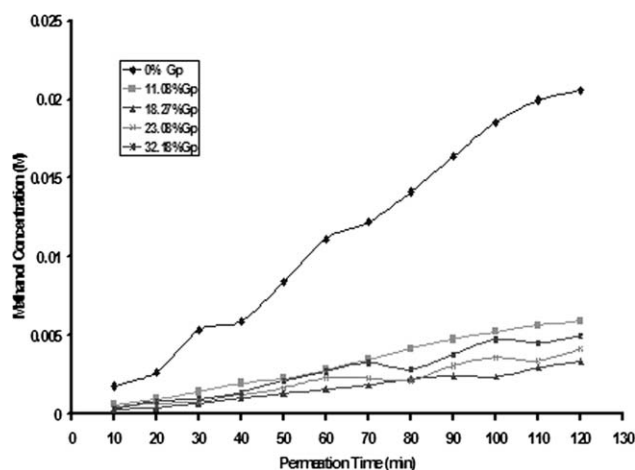


**Figure 16** Variation of the methanol concentration for the modified membranes with different GP% values in comparison with the virgin Nafion as a function of the permeation time.

we found that there was no significant reduction in the methanol permeability with grafted polymer contents higher than 18.27%. From the results represented here, the reduction in the methanol permeability may have been due to the incorporation of PGMA into the Nafion matrix, which led to a decrease in the ion channels of the modified membrane compared to those of the virgin Nafion and, therefore, overcame the methanol crossover drawback. The results were in agreement with many published data.<sup>9,10</sup>

**Membrane efficiency.** To evaluate the efficiency of the modified membranes, we compared their characteristic factor, which was the ratio between IEC and methanol permeability as an indicator of membrane performance in DMFC<sup>33,34</sup> according to eq. (12). The efficiency factor of the modified membranes in comparison with the virgin Nafion membrane is represented graphically as function of the grafted polymer content in Figure 18. As shown in Figure 18, the efficiency factor for all of the modified membranes was higher than that of ungrafted Nafion. The maximum value was obtained with a GP% of 18.27%. This made the modified Nafion more attractive for application in DMFCs because its efficiency increased by a factor of 4 with a GP% of 18.27%.

## CONCLUSIONS

Modified Nafion membranes for DMFCs were prepared and characterized. Through the membrane preparation process, we functionalized Nafion membranes through grafting with PGMA using a persulfate initiation system. The effects of different factors, such as the monomer, initiator concentration, time, temperature, and solvent ratio, on the grafting parameters were studied. The grafting process was controlled through variation of the grafting conditions, and as a result, different GP%'s were obtained.

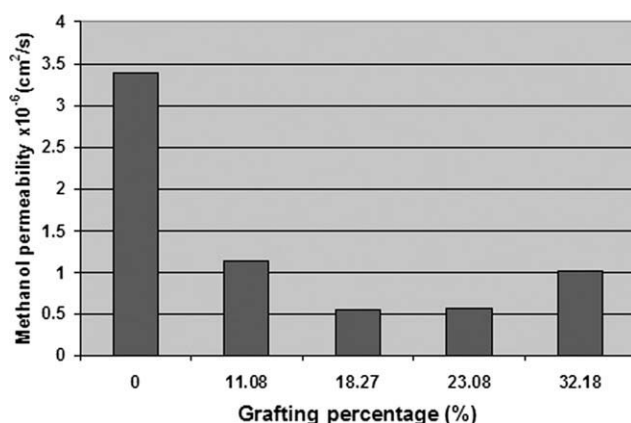


**Figure 17** Effect of GP% on the permeability of the modified membranes in comparison with the ungrafted Nafion membrane.

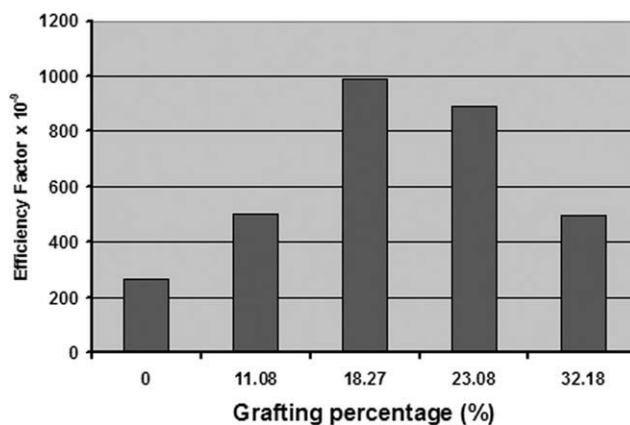


**Figure 18** Comparison of the efficiency factor for the modified membranes with different GP% values and the ungrafted Nafion membrane.

The occurrence of grafting was proven by FTIR spectroscopy, TGA, and SEM. The introduced epoxy groups of PGMA were subsequently converted into amine groups by the amination process with EDA. Doping phosphoric acid ( $-\text{PO}_3\text{H}$ ) groups to the amino side chains of the grafted membranes significantly contributed to the enhancement of the thermal stability and the mechanical properties of the Nafion modified membranes. The thickness of the grafted membranes increased with increasing GP%. The methanol permeability of modified membranes decreased with increasing grafted polymer content by about 84% compared to the virgin Nafion. As a result, the efficiency factor for all of the modified membranes was higher than that of ungrafted Nafion. The maximum value was obtained with a GP% of 18.27%. The combination of the obtained results makes the modified Nafion more attractive for application in DMFCs.

## References

- Larminie, J.; Dicks, A. *Fuel Cell Systems Explained*; Wiley: New York, 2000; Chapter 1.
- Prater, K. *J Power Sources* 1990, 29, 239.
- Some History on Fuel Cells; Bear, Stearns Distributed Energy Services: Annual Report 2001.
- Scott, K.; Taama, M.; Argyropoulos, P.; Sunmacher, K. *J Power Sources* 1999, 83, 204.
- Jeon, W.; Sriram, V.; Sung, K. *Polym Int* 2006, 55, 491.
- Nagarale, K.; Gohil, S.; Shahi, K. *J Membr Sci* 2006, 280, 389.
- Tsai, J. C.; Kuo, J. F.; Chen, C. Y. *J Power Sources* 2007, 174, 103.
- Wen, S.; Gong, C.; Tsen, W.; Shu, Y.; Tsai, F. *J Appl Polym Sci* 2010, 116, 1491.
- Sank, J.; Byun, J.; Kim, H. *J Power Sources* 2004, 132, 59.
- Bae, B.; Yong Ha, H.; Kim, D. *J Membr Sci* 2006, 276, 51.
- Ren, S.; Sun, G.; Li, C.; Song, S.; Xin, Q.; Yang, X. *J Power Sources* 2006, 157, 724.
- Bebin, P.; Caravanier, M.; Galiano, H. *J Membr Sci* 2006, 278, 35.

13. Sacca, A.; Carbone, A.; Passalacqua, E.; D'Epifano, A.; Licocchia, S.; Traversa, E.; Sala, E.; Traini, F.; Orneltas, R. *J Power Sources* 2006, 152, 16.
14. Kim, Y. T.; Kim, K. H.; Song, M. K.; Rhee, H. W. *Curr Appl Phys* 2006, 6, 612.
15. Costamagna, P.; Yang, C.; Bocarsly, A. B.; Srinivasan, S. *Electrochim Acta* 2002, 47, 1023.
16. Damay, F.; Klein, L. C. *Solid State Ionics* 2003, 162–163, 261.
17. Cho, K. Y.; Jung, H. Y.; Shin, S. S.; Choi, N. S.; Sung, S. J.; Park, J. K.; Choi, J. H.; Park, K. W.; Sung, Y. E. *Electrochim Acta* 2004, 50, 589.
18. Guo, W.; Zhao, S.; Prabhuram, J.; Wong, W. *Electrochim Acta* 2005, 50, 1973.
19. Mohy Eldin, M. S.; Soliman, E. A.; Hassan, E. A.; Abu-Saied, M. A. *J Appl Polym Sci* 2009, 111, 2647.
20. Nasef, M. M.; Zubir, N. A.; Ismail, A. F.; Khayet, M.; Dahlan, M.; Saidi, H.; Rohani, R.; Ngah, S.; Sulaiman, N. A. *J Membr Sci* 2006, 268, 96.
21. Masahiro, R.; Daisuke, I.; Keiichi, K.; Yuko, T.; Iko, I.; Yoshio, K.; Kohei, S. *J Mol Struct* 2005, 739, 153.
22. Nasef, M. M.; Zubir, N. A.; Ismail, A. F.; Dahlan, K. Z. M.; Saidi, H.; Khayet, M. *J Power Sources* 2006, 156, 200.
23. Commer, P.; Cherstvy, A. G.; Spohr, E.; Kornyshev, A. A. *Fuel Cells* 2003, 3, 127.
24. Junfeng, Z.; Koichi, K.; Yoshikimi, U.; Yoshito, I. *J Polym Sci Part A: Polym Chem* 1995, 33, 2629.
25. Lagarón, J. M.; Giménez, E.; Gavara, R.; Saura, J. J. *Polymer* 2001, 42, 9531.
26. Jacobus, K.; Freek, A.; Brinkman, U.; Gooijer, C. *Anal Chim Acta* 2003, 488, 135.
27. Guadalupe, I.; Gustavo, V.; Barbosa, C. *Food Sci Technol* 2008, 41, 359.
28. Qíngfeng, L.; Ronghuan, H.; Rolf, B.; Hans, A. H.; Niels, J. B. *Solid State Ionics* 2004, 168, 177.
29. Gang, L.; Xiulin, Z.; Jian, Z.; Zhenping, C.; Wei, Z. *Polymer* 2005, 46, 12716.
30. Nikhil, H. J.; Katherine, D.; Ravindra, D. *Electrochem Acta* 2005, 51, 553.
31. Becker, W.; Schmidt, G. *Chem Eng Technol* 2002, 25, 373.
32. Jongok, W.; Sang, C.; Yong, K.; Heung, H.; Hwan, O.; Hoon, K.; Kyoung, K.; Won, J. *J Membr Sci* 2003, 214, 245.
33. Masanobu, M.; Heisuke, T. *J Membr Sci* 2006, 281, 707.
34. Bae, B.; Yong, H.; Kim, D. *J Electrochem Soc* 2005, 152, A1366.